



Thermal decomposition of 1-pentyl radicals at high pressures and temperatures

Andrea Comandini^{a,1}, Iftikhar A. Awan^b, Jeffrey A. Manion^{b,*}

^a Department of Mechanical Engineering, University of Illinois at Chicago, Chicago, IL 60607, USA

^b Chemical and Biochemical Reference Data Division, National Institute of Standards and Technology, Gaithersburg, MD 20899-8320, USA

ARTICLE INFO

Article history:

Received 3 July 2012

In final form 20 September 2012

Available online 27 September 2012

ABSTRACT

Shock-tube studies at the National Institute of Standards and Technology (NIST) and the University of Illinois at Chicago (UIC) have been used to examine the decomposition of 1-pentyl radicals in argon between (833–1130) K and (100–5000) kPa. High pressure limiting values of the product branching ratios appear to be approached at the highest pressures studied. Results agree well with a ‘best-fit’ model previously developed [1] and are consistent with an energy transfer value $\langle \Delta E_{\text{down}} \rangle = (675 \pm 100) \text{ cm}^{-1}$ at 1000 K.

Published by Elsevier B.V.

1. Introduction

The decomposition of alkyl radicals plays a prominent role in the combustion of hydrocarbon fuels. Under conditions of interest there is a competition between bimolecular oxidation reactions and unimolecular processes that fragment or isomerize the fuel radical. The competition between these processes is a determinant of the product mix in the initial breakdown of a fuel and this is responsible for many of the observed differences and similarities in the burning characteristics of fuels.

The 1-pentyl radical is the smallest alkyl radical that can undergo a five center intramolecular H transfer reaction that alters the position of the radical center. Its decomposition has been studied for many years, both experimentally [1–7] and theoretically [8–14]. Recent measurements carried out at NIST [1] were the first to experimentally probe the olefin product branching ratio determined by the competition between isomerization and beta C–C bond scission. The ratio was found to be temperature and pressure dependent. A Rice-Ramsberger-Kassel-Marcus/Master Equation (RRKM/ME) analysis was carried out and the experimental results were compared with quantum chemical calculations. While qualitative agreement between experiment and computation was achieved, it proved necessary to modify the computed potential energy surface (PES) in order to match the experimental data. A ‘best fit’ model was ultimately constructed on the basis of a critical analysis of the product branching ratio data together with consideration of relevant literature data from kinetic experiments at lower temperatures. A key quantity was the variation of the product ratio with pressure, and the experimental results placed significant constraints on the PES and the value of the energy

transfer parameter used in conjunction with the model and the RRKM/ME analysis.

The above experiments were carried out at pressures ranging from about 80 to 600 kPa. Limitations in the shock-tube prevented the extension to higher pressures. Significant differences in the computed variation of the product branching ratio with pressure and its high pressure limiting value were obtained when using the computed PES compared with the empirically adjusted ‘best-fit’ model. While potential sources of systematic error in the experiments were considered, the pressure range over which data could be taken was limited and this increases the possibility that small perturbations could impact the results. The presently described experiments represent an attempt to further test the models by extending the range of pressure over which data are available. To that end, the high-pressure shock tube at the University of Illinois at Chicago (UIC) has been employed to carry out experiments at pressures as high as 5000 kPa and these data are compared with NIST measurements taken at lower pressures.

2. Experimental procedures

2.1. NIST apparatus and procedures

Previous publications [15,16] have described the single-pulse shock tube used at NIST in detail. In brief, samples are prepared in 15 L holding tanks using calibrated capacitance manometers. Shocks are generated by rupture of a cellophane diaphragm and samples of the post-shock gases are withdrawn for immediate analysis using a valve and loop sampling system that is directly interfaced with the shock tube. The shock tube, sample preparation system, and the analytical system are heated to typically 373 K throughout to maintain heavier components in the gas phase. The configuration of the shock tube results in heating times, as derived from recorded pressure traces, of $(500 \pm 50) \mu\text{s}$, and the shock pressures that are attainable are roughly 80–750 kPa.

* Corresponding author. Fax: +1 (301) 869 4020.

E-mail address: jeffrey.manion@nist.gov (J.A. Manion).

¹ Present address: Institut de Combustion, Aérothermique, Réactivité et Environnement, Centre National de la Recherche Scientifique, 45071 Orléans, France.

The postshock gas analysis employs an Agilent Technologies 6890N gas chromatograph (GC) equipped with a Restek 30 m × 0.53 mm i.d. Rt-Alumina (aluminum oxide porous layer) capillary column for hydrocarbons up to about C5 and a J&W Scientific DB-1 30 m × 0.53 mm internal diameter (i.d.) fused silica capillary column for the heavier species. [Disclaimer: Certain commercial materials and equipment are identified in this Letter in order to specify adequately the experimental procedure. In no case does such identification imply recommendation or endorsement by the National Institute of Standards and Technology, nor does it imply that the material or equipment is necessarily the best available for the purpose.] The GC is equipped with both flame ionization detection (FID) and an Agilent Technologies 5973 Inert mass selective detector. An Agilent Technologies microfluidic splitter based on differential pressures (Dean's Switch) is used to quantitatively split the sample eluting from the DB-1 column to allow simultaneous identification and quantification of the mixture components by mass spectrometry and FID analysis. The GC oven can be cooled with chilled nitrogen gas, and the present analyses utilize an oven temperature program spanning 213–453 K. The cryogenic conditions allow the DB-1 column to adequately separate many of the smaller species determined with the Rt-alumina column. In cases where analyses were possible on both columns, derived amounts agreed typically within a few percent. FID responses of all major olefin products were determined from standard samples and should be accurate to within 5%. Values for some minor products were estimated based on carbon number and standard FID response relationships. These should be accurate to about 10%. Peak areas were determined using the HP ChemStation software.

Shock temperatures are determined using a comparative rate technique whereby we follow the progression of an internal standard reaction that proceeds with a known rate constant. The present experiments make use of the decomposition of the substrate itself for this purpose. The rate expression $k(1\text{-iodopentane} \rightarrow \text{Products}) = 10^{13.96} \exp(-24513/T) \text{ s}^{-1}$ was determined in our previous work (1) relative to $k_{\text{c}}(\text{chlorocyclopentane} \rightarrow \text{cyclopentene} + \text{HCl}, 590\text{--}1020 \text{ K}) = 10^{13.75} \exp(-24514/T) \text{ s}^{-1}$. The rate expression for chlorocyclopentane is from our recent comprehensive study [17] and critical evaluation of several temperature standards. Since the relative values for 1-iodopentane and chlorocyclopentane are based on direct competitions, it will be possible to directly compare the present data with those from our previous study of 1-pentyl radical, in which chlorocyclopentane was used as the temperature standard. We estimate the standard uncertainties (1σ) in the absolute temperatures to be about $\pm 10 \text{ K}$.

2.2. University of Illinois at Chicago apparatus and procedures

The single-pulse high-pressure shock tube (HPST) present at the University of Illinois at Chicago (UIC) has been described in detail in earlier publications [18–20]. Therefore only the relevant features are reported here. The HPST consists of a 297 cm (117 in.) long driven section with an inner diameter of 2.54 cm (1 in.) and a driver section with an inner diameter of 5.08 cm (2 in.). The length of the driver section is varied by inserting metallic plugs in order to obtain constant reaction conditions as well as fast cooling of the reaction by the rarefaction wave. Nominal post-shock pressure conditions of 2500 and 5000 kPa were obtained utilizing 0.0635 cm (0.025 in.) thick aluminum diaphragms with score depths of 0.0254 cm (0.010 in.) and 0.0127 cm (0.005 in.) respectively. Reagent mixtures are prepared manometrically in 42 L vessels and allowed to stand overnight before use. The entire apparatus is heated to 373 K.

A high-frequency PCB piezoelectric pressure transducer is mounted on the end-wall of the driven section perpendicularly to

the flow. The corresponding pressure trace was used in order to determine both the experimental pressure and the reaction time which is defined as the time between the arrival of the incident wave at the end-wall and the time when the pressure reaches the 80% of its maximum value [21]. Uncertainty in the time measurement is no more than 10%. Six additional PCB transducers are positioned along the driven section for the measurement of the incident shock wave velocities. Such velocities are experimentally related to the temperatures in the post-shock reaction by means of external chemical thermometers [19]. The presently described experiments encompass a temperature range of 300 degrees. The most reliable temperatures from the standards are obtained at moderate degrees of conversions, which necessitates the use of several chemical thermometers to cover the entire range. The standards used for calibration of the low, intermediate and high temperature regimes were respectively 1-iodopentane(1), $\approx (830\text{--}900 \text{ K})$, chlorocyclopentane [17] and cyclopropanecarbonitrile [22], $\approx (900\text{--}1030 \text{ K})$, and 1,1,1-trifluoroethane [23], $\approx (1030\text{--}1130 \text{ K})$. Temperatures derivable from the various standards were in good agreement in the overlapping temperature regions. The estimated uncertainty in the postshock temperature is about 1%.

A sample of gas is withdrawn from the post-shock mixture through an automated sampling apparatus. The sampling apparatus is coupled directly to the analytical system for the measurement of the stable products. Neon is added to the mixtures as an internal standard to account for any dilution by the driver gas. The analytical system consists of two Hewlett–Packard 6890 series gas chromatographs, the first equipped with a FID detector connected to a DB-17 ms column for the measurement of 1-iodopentane, the second GC equipped with a FID detector and a TCD detector connected respectively to an HP-PLOT Q column for measurement of light species and to a HP-PLOT MoleSieve column for measurement of inert gases. An Agilent Technologies 5973 series mass spectrometer is also connected to the second GC for identification of unknown products. The GC calibration for the major gas components was performed using certified gas mixtures as well as in-house prepared calibration mixtures. Typical uncertainties in the measurement of such species are about 5%. Calibration curves for some minor products were estimated based on the carbon number. The corresponding uncertainties should be no more than 10%.

2.3. Chemicals

Chemicals used in the present mixtures were 1-iodopentane (98%, Aldrich), and high-purity Argon [99.999%, Praxair (NIST) or Airgas (UIC)]. The argon was further purified with a Matheson oxygen filter (UIC) or Restek thermal gas purifier (NIST). Primary impurities in the NIST sample of 1-iodopentane were determined to be 1-bromopentane (1.6%) and 1-chloropentane (0.3%) by GC/MS analysis. The UIC sample was not tested, but was from the same company and had the same nominal purity. Chemicals were degassed with standard freeze, pump, thaw techniques prior to use.

3. Results and discussion

The basis of our methodology is to use an appropriate precursor to create the radical of interest under very dilute conditions where it can undergo only unimolecular decomposition reactions. These reactions lead to a distribution of stable olefin products that correspond to the initial fragmentation pattern of the radical. The olefins are observed in postshock analyses and the cracking pattern then related to the precursor radicals and the kinetics of the competing reactions. In the present instance we generate the 1-pentyl radical from the thermal decomposition of 1-iodopentane.

3.1. Product distribution and mechanism

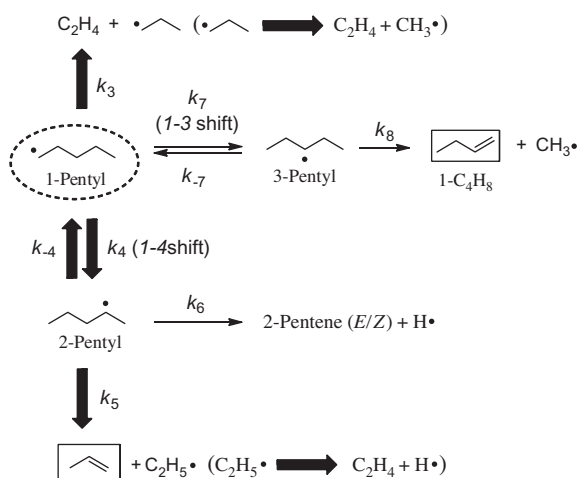
Product data from individual experiments are provided in [Supplementary Tables S1 and S2](#). The mechanism and kinetics of the unimolecular decomposition of 1-iodopentane has been investigated in our previous work (1): it proceeds via both fission of the weak C–I bond and molecular elimination of HI:



Under our conditions the former process accounts for about 75% of reaction. It is therefore an effective source of the 1-pentyl radical. Rate constants for decomposition of the 1-pentyl radical [1] entail a lifetime of about 0.1 μs near 1000 K, so that bimolecular reactions cannot compete with its unimolecular decomposition under our dilute conditions. The shocked gas is heated for typically 300–500 μs and the olefin decomposition products are quite stable on this time scale. Also noteworthy is that the product spectrums from channels (1) and (2) do not overlap, allowing the decomposition reactions of the radical to be isolated.

1-Pentene is the olefin product corresponding to molecular loss of HI, reaction (2). The decomposition chemistry of the 1-pentyl radical is summarized by reactions (3) to (8) in [Scheme 1](#). The predominant olefin products are ethene and propene, but very small amounts (<1% of the total olefin yield) of 1-butene, (*E*)-2-pentene, and (*Z*)-2-pentene are also observed. [Scheme 1](#) does not indicate possible 1–2 and 2–3 H shift reactions, which have been shown to be of very minor importance. (1,12) More detailed discussion of the mechanism and possible impact of minor channels is given in our other works [1,24]. Presently we emphasize that the ethene to propene product ratio is determined in large part by the kinetics of beta C–C bond scission (k_3) relative to the 1–4 isomerization (k_4). It is the pressure dependence of this product ratio that is the primary focus of the present Letter.

The previous NIST study utilized mixtures containing small amounts (50–300) $\mu\text{L/L}$ of the iodide in the presence of a large excess (5000 $\mu\text{L/L}$) of a radical scavenger, either *m*-xylene or 1,3,5-trimethylbenzene. In the present experiments we take a different approach, and have removed all organic components other than the iodide, which is added to the argon bath gas at very low levels of typically 50 $\mu\text{L/L}$. This assures that all observed olefins are products derived from the starting substrate. The remaining question is



Scheme 1. Main product pathways postulated for the decomposition of 1-pentyl radicals. Paths indicated by non-block arrows have branching ratios of <1%. The starting radical is indicated by the dashed oval. Products linked to a specific pentyl radical isomer are enclosed in boxes.

whether or not the measured ethene/propene ratios are significantly impacted by processes other than unimolecular decomposition of the 1-pentyl radical. In essence we are assuming that radical-induced decomposition of the substrate is minimal and thus that iodide decomposition is a self-inhibiting system. There are strong reasons to think that this might be the case since the iodides are well-known [25,26] to inhibit flame chemistry by catalytic cycles that remove active species such as H atoms and replace them with weakly reactive I atoms:



Similar processes will help remove relatively long-lived alkyl radicals, such as methyl, that lack facile unimolecular modes of decomposition:



The HI bond strength is only 298 kJ mol^{-1} [27], so that attack of I on a typical C–H bond, reaction 15, is endothermic by more than 110 kJ mol^{-1} .



Consequently such reactions are slow and iodine atoms are poor propagators of radical chain reactions. The expectation is that the net effect is to effectively inhibit radical chain processes. If this is the case, measured ethene/propene ratios correspond directly with the decomposition behavior of the 1-pentyl radical. Evidence for this supposition is examined below, and includes an empirical test where ratios are compared with previous results, and an analysis of secondary products for indications of more complex chemistry.

Empirically, new experiments were carried out at NIST with mixtures that contained only 40 $\mu\text{L/L}$ iodopentane and argon under pressure conditions that matched those of our previous study, wherein the mixtures contained large amounts of a methylbenzene inhibitor. The newly measured ethene/propene ratios, determined at two sets of pressures of roughly 200 and 600 kPa, fall precisely on the lines found previously (*vide infra*, Section 3.2). This is suggestive that there are no significant perturbations of the ethene/propene ratio due to the absence of an additional inhibitor. Corresponding experiments with iodopentane/argon-only mixtures were performed at higher pressures with the UIC shock tube. Two sets of pressure conditions, roughly 2250 and 5000 kPa, were examined. To further test the consistency of the data, the UIC experiments were completed with iodide concentrations near both 50 and 100 $\mu\text{L/L}$. [Figure 1](#) compares the ethene/propene ratios obtained in these experiments. Within the scatter, the change in the iodide concentration has no discernible impact in the ethene/propene ratio.

Secondary products provide an additional test of our assumptions. Secondary chemistry in the pentyl iodide system is minor in the presence of an inhibitor, and a detailed discussion has been provided in our previous work (1). We presently limit ourselves to the most relevant observations with respect to the iodide-only experiments carried out at UIC. Under those conditions ethane is found at levels of (3–5)% of ethene, while methane increases from about 5% of ethene near 850 K to about 20% near 1050 K. Ethane is the result of the self-recombination of CH_3 produced in the decomposition of pentyl radicals ([Scheme 1](#)), while H-abstraction reactions by methyl, e.g. reaction 12, are the source of methane. The

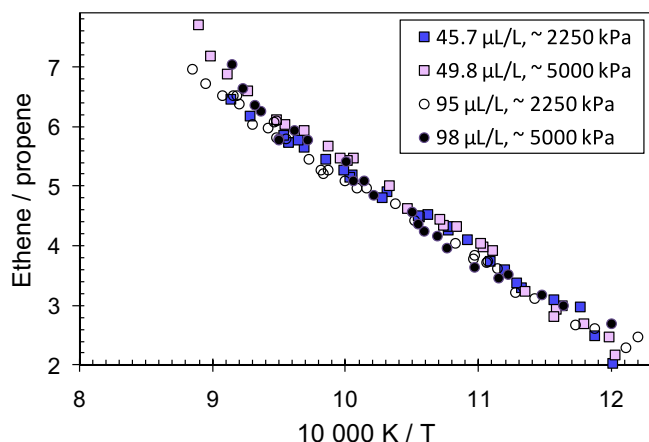
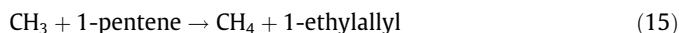
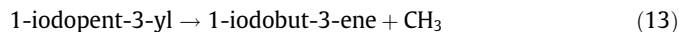
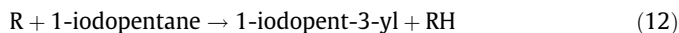


Figure 1. Comparison of ethene/propene ratios obtained in experiments at UIC with the concentration of the starting changed from approximately (50–100) $\mu\text{L/L}$.

main question is possible interference by attack of methyl radicals on the starting iodide:

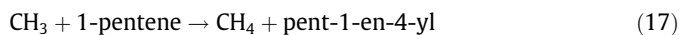


At higher temperatures small amounts of 1,3-butadiene are observed. This product, not noted in our previous lower-pressure study where an inhibitor was used, suggests a degree of radical attack on the starting iodide (reactions 18–20) or the 1-pentene product of HI elimination (reactions 21 and 22):



1,3-Butadiene was first detectable in the UIC studies near 950 K, where it is present at a level of about 0.1% of ethene. Relative to ethene formation, amounts of 1,3-butadiene increase both with the shock pressure and with the starting iodide concentration. When $\approx 50 \mu\text{L/L}$ of the starting iodide is used, 1,3-butadiene increases from 2% to 3% of ethene at 1050 K as the pressure is increased from 2300 to 5000 kPa. If the shock pressure is maintained at ≈ 2300 kPa, a similar increase is observed when the concentration of the starting iodide is increased from 46 to 95 $\mu\text{L/L}$. Levels of 1,3-butadiene ultimately reach about 7% of ethene near 1130 K, the highest temperature studied.

Another product suggestive of radical-induced chemistry is 1,3-pentadiene. It is present at levels that are generally lower than 1,3-butadiene, and increases from about 0.1% to 1.0% of ethene between 950 and 1130 K. It can be formed via:



The above observations suggest that radical induced decomposition is relatively minor, but plays an increasing role at the upper end of our temperature range. At the lower pressures covered by the NIST data there are no appreciable differences in ethene/propene ratios obtained with and without an added methylbenzene

inhibitor. Ideally data under both sets of conditions would also be available at the higher pressures of the UIC experiments, and we hope to be able to make some comparisons in future work. The data in hand are nonetheless convincing. Our analysis would suggest, however, that the data from higher temperatures, say above 1025 K, are more subject to interference from radical-induced decomposition.

3.2. Pressure dependence of the product ratios

3.2.1. Ethene/propene ratio

Figure 2 presents a plot that shows the pressure effect on the ethene/propene ratio. Included are the new UIC and NIST data, together with predictions from our master equation RRKM analysis. Individual points from the previous NIST experiments(1) are not specifically shown in the present report, but are well described by the dashed curves. For clarity, the UIC data are plotted only for the experiments utilizing $\approx 45 \mu\text{L/L}$ of the starting iodide. These lower-concentration experiments are expected to be less impacted by possible systematic effects than are the results at 100 $\mu\text{L/L}$, although Figure 1 shows that any concentration dependence is small. The RRKM results are obtained with the ChemRate software package [8,28–30]. Our model assumes a continuous incoming flux of the 1-pentyl radical at the temperature of the bath gas. The master equation is then solved with an eigenvalue/eigenvector approach [29–31] to obtain a time-dependent evolution of the species and their energies. Steady-state distributions and stable branching ratios are computed to be reached within about 1×10^{-5} s under our experimental conditions. The present results are based on the ‘best-fit’ PES developed in reference [1]. Stationary point energies and molecular properties of species in that model were derived initially from quantum chemical calculations, and then critically adjusted to fit both the NIST product branching ratio data at $\approx (90\text{--}600)$ kPa, and relevant literature data from kinetic experiments at lower temperatures. Energy transfer is described with an exponential-down model [31], with $\langle \Delta E_{\text{down}} \rangle / \text{cm}^{-1} \text{K}^{-1} = 0.675T$, where T is the temperature in Kelvin. Tunneling is included via an asymmetric Eckart potential adjusted to provide a good fit to lower temperature kinetic data. More discussion is provided in our previous report [1]. To account for the slight temperature dependence of the experimental shock pressures, pressure versus temperature plots were used to select the conditions used

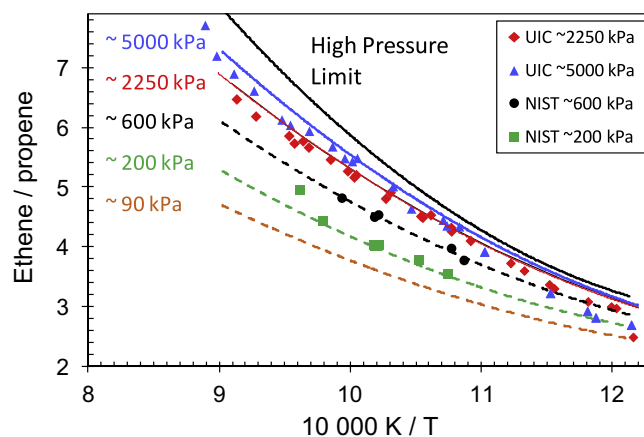


Figure 2. Pressure dependence of the ethene/propene product ratio in the decomposition of 1-pentyl radicals. Symbols indicate new experimental points from the present Letter. Lines indicate predictions based on the ‘best-fit’ model developed in Ref. [1]. Individual points from the previous work at pressures of 90–600 kPa are not shown, but are well-represented by the dashed curves. Approximate pressures are as indicated. Computed ratios for specific conditions are given in Table 1.

for the model predictions given in Figure 2. Computed ratios for specific conditions are given in Table 1.

Some small improvements have been made to the ‘best fit’ model presented in Ref. [1]. For completeness we have added minor C–H bond scission channels. The kinetic parameters reflect our recent work on the addition of H to (*E*)-2-pentene [24], which applies through detailed balance. The C–H bond scissions play almost no role under the conditions studied in the present experiments <2%, see products in Tables S1 and S2, but are predicted to have a minor impact as the model is extrapolated to higher temperatures. Additionally, in the course of preparing the present Letter it was discovered that the electronic degeneracy of the activated complex for reaction 3 (Scheme 1) was inadvertently set as 1 rather than 2. This impacts the pre-exponential factor and requires a readjustment of the lowest frequency of the complex in our ‘best fit’ model to recover the rate constants and fit reported previously (note that this same frequency was empirically adjusted in Ref. [1] as part of the fitting procedure). Compared with Ref. [1], computed branching ratios are altered by less than 0.5% in the experimental temperature range, and by no more than a few percent over the entire range of conditions considered. These differences are similar or less than numerical round-off errors in the calculations, and the parameterized rate constants presented in Ref. [1] are almost indistinguishable from the present values. The updated high pressure limiting rate parameters, including new estimations for C–H scission channels, are given in Table 2. For purposes of chemical modeling,

in the Supplementary material we additionally provide parameterizations of the computed pressure-dependent rate constants in the PLOG format used by ChemKin Pro [32]. Results are those obtained when the 1-pentyl radicals are initially created with a thermal (Boltzmann) distribution. They cover (600–1700) K and (10–100 000 kPa) and represent values derived after steady-state energy distributions are reached, typically within 1×10^{-5} s.

Figure 2 shows there is noticeable roll-off in the experimental ratio observed below about 900 K, with progressively larger deviations from the predicted values at lower temperatures. Temperatures in this region were based on the rate parameters for decomposition of 1-iodopentane from Ref. [1]. Errors due to extrapolation of the rate parameters or pressure effects thereon could possibly account for some of the discrepancy. Notice also, however, that at the lowest temperatures the product ratios at 5000 kPa appear to fall below those at 2250 kPa, which is not as expected. At present this behavior is not fully understood. One speculation is that the experimental data are increasingly affected by contributions from bimolecular reactions as the radical lifetimes increase rapidly at lower temperatures. In unpublished work, similar low-temperature behavior has been observed at NIST in studies of the decomposition of other alkyl radicals, although at the lower pressures of the NIST studies the roll-off occurs at temperatures lower than shown by the UIC data. A dependence on pressure would be consistent with expectations for bimolecular processes, wherein reaction rates scale with concentrations squared.

Table 1
Computed ethene/propene ratios in the decomposition of 1-pentyl radicals as derived from the RRKM/ME models described in the text. Pressure/temperature combinations correspond to approximate average values for the sets of conditions examined experimentally.

Corresponding Experiments	Temp (K)	Pressure (kPa)	Computed ethene/propene ratio	
			‘Best fit’ PES $\alpha = 0.675T^a$	<i>a priori</i> PES $\alpha = 0.100T^b$
NIST low-pressure data sets	860	71	2.68	2.58
	900	79	2.97	2.89
	940	87	3.28	3.24
	980	95	3.60	3.64
	1020	103	3.93	4.10
NIST mid-pressure data sets	1050	109	4.20	4.49
	860	154	2.91	3.08
	900	165	3.24	3.45
	940	179	3.60	3.87
	980	196	3.97	4.35
NIST high-pressure data sets	1020	215	4.37	4.91
	1050	232	4.68	5.39
	860	448	3.18	3.94
	900	494	3.60	4.49
	940	542	4.05	5.08
UIC lower pressure data sets	980	594	4.51	5.74
	1020	649	4.99	6.46
	1050	693	5.37	7.05
	860	2222	3.44	5.51
	900	2237	3.94	6.27
UIC higher pressure data sets	940	2252	4.47	7.06
	980	2267	5.02	7.87
	1020	2283	5.58	8.71
	1050	2294	6.01	9.37
	860	4785	3.50	6.30
Computed high pressure limits	900	4868	4.03	7.28
	940	4951	4.61	8.29
	980	5034	5.22	9.33
	1020	5118	5.85	10.40
	1050	5180	6.34	11.22
	860	1×10^8	3.56	9.09
	900	1×10^8	4.14	11.32
	940	1×10^8	4.79	13.88
	980	1×10^8	5.48	16.77
	1020	1×10^8	6.24	19.96
	1050	1×10^8	6.84	22.55

^a Includes tunneling correction, PES = potential energy surface, $\alpha = \langle \Delta E_{\text{down}} \rangle / \text{cm}^{-1} \text{K}^{-1}$ = energy transfer parameter.

^b Includes tunneling correction; the value of $\langle \Delta E_{\text{down}} \rangle$ was selected so as to match the experimental ethene/propene ratios at the lowest pressures studied.

Table 2

Limiting high pressure rate expressions for 1-pentyl radical decomposition. Significant figures are reported to adequately represent the model results and do not imply accuracy.

Reaction #	Reaction	Log A	n	E (K)	Log k_{∞} (1000 K)
<i>A: High pressure limiting rate expressions: $k_{\infty}(400\text{--}1900\text{ K}) = A T^n \exp(-E/T) \text{ s}^{-1}$</i>					
k_3	1-Pentyl \rightarrow ethene + <i>n</i> -propyl	12.51	0.323	14497	7.18
k_5	2-Pentyl \rightarrow ethyl + propene	2.61	0.272	14664	7.06
k_8	3-Pentyl \rightarrow 1-butene + methyl	10.47	0.928	15121	6.69
k_4	1-Pentyl \rightarrow 2-pentyl	1.06	3.033	7706	6.81
k_{-4}	2-Pentyl \rightarrow 1-pentyl	-0.631	3.533	9049	6.04
k_7	1-Pentyl \rightarrow 3-pentyl	-11.41	6.843	9451	5.02
k_{-7}	3-Pentyl \rightarrow 1-pentyl	-13.50	7.515	10736	4.38
k_{25}	2-Pentyl \rightarrow 3-pentyl	10.44	0.712	21071	3.43
k_{-25}	3-Pentyl \rightarrow 2-pentyl	10.04	0.884	21013	3.56
k_{26}	1-Pentyl \rightarrow 1-pentene + H	10.31	0.950	17014	5.77
k_{6a}	2-Pentyl \rightarrow <i>E</i> -2-pentene + H	9.06	1.220	17239	5.24
k_{6b}	2-Pentyl \rightarrow <i>Z</i> -2-pentene + H	9.69	1.028	17683	5.09
k_{27}	2-Pentyl \rightarrow 1-pentene + H	8.35	1.517	17487	5.31
k_{28}	3-Pentyl \rightarrow <i>E</i> -2-pentene + H	8.66	1.379	17166	5.34
k_{29}	3-Pentyl \rightarrow <i>Z</i> -2-pentene + H	9.72	1.061	17745	5.19
<i>B: Addition reactions (from detailed balance): $k_{\infty}(400\text{--}1900\text{ K}) = A T^n \exp(-E/T) \text{ cm}^3 \text{ mol}^{-1} \text{ s}^{-1}$</i>					
k_{-3}	Ethene + <i>n</i> -propyl \rightarrow 1-pentyl	2.45	2.841	2591	9.85
k_{-5}	Ethyl + propene \rightarrow 2-pentyl	3.52	2.451	2983	9.58
k_{-8}	1-Butene + methyl \rightarrow 3-pentyl	4.08	2.393	2634	10.12
k_{-26}	1-Pentene + H \rightarrow 1-pentyl	9.08	1.323	528	12.82
k_{-27}	1-Pentene + H \rightarrow 2-pentyl	8.82	1.389	-341	13.13
k_{-6a}	<i>E</i> -2-Pentene + H \rightarrow 2-pentyl	8.46	1.506	344	12.82
k_{-28}	<i>E</i> -2-Pentene + H \rightarrow 3-pentyl	8.45	1.494	329	12.79
k_{-6b}	<i>Z</i> -2-Pentene + H \rightarrow 2-pentyl	8.14	1.596	245	12.82
k_{-29}	<i>Z</i> -2-Pentene + H \rightarrow 3-pentyl	8.58	1.458	365	12.79

As indicated in the above discussion, experiments at the lower end of our temperature range can be impacted by bimolecular processes, while radical-induced decomposition may have some influence at the upper end: the most reliable results are expected in the intermediate range of roughly 900–1025 K. In this range the new UIC data at 2250 and 5000 kPa fall about 3% lower than the model predictions. As discussed in detail in our previous publication [1], the NIST data contain small corrections to the ethene concentrations due to formation of ethyl and propyl iodides. These corrections amount to (1–6)% in the present NIST experiments (see Table S2). Due to differences in the columns used in the GC analyses, the iodides were not observed in the UIC experiments and these corrections were not employed in the UIC data. Their inclusion would tend to increase the UIC ethene/propene ratios by a small percentage. Overall, we estimate that the experimental uncertainty in the UIC branching ratio data, including analytical uncertainties and systematic perturbations due to secondary chemistry, is about 10%. Given this, the level of agreement with the ‘best-fit’ model is remarkably good.

Previously we tested some alternative models using an unadjusted potential energy surface derived from calculations at the G3MP2B3 level of theory. Inclusion of tunneling improved the fit, but to match the experimental C2/C3 ratios these models required much smaller values of $\langle\Delta E_{\text{down}}\rangle$ than those used in our ‘best fit’ model. After correction of the electronic degeneracy term for reaction 3 alluded to earlier, a fit to the observed low pressure ratios when using our *a priori* model with tunneling included requires $\langle\Delta E_{\text{down}}\rangle \approx 100 \text{ cm}^{-1}$ at 1000 K. Extrapolation to the high pressure limit then results in ethene/propene ratios about a factor of three larger than indicated by the present data (see Table 1 for computed ratios). Such models are obviously not supported.

3.2.2. Ratios of the minor products

In our earlier study, 1-butene, (*E*)-2-pentene and (*Z*)-2-pentene were found as very minor products, with product branching ratios of <0.01. These same species are observed at similar levels in the present experiments. We previously noted that these very minor channels are more subject to interference from secondary chemistry

than are the main propene and ethene channels. In the [Supplementary material](#) we provide product amounts for the minor species. The present data are generally consistent with the results from our previous study at lower pressures, but show some divergence at the temperature extremes. This may suggest some impact from bimolecular and radical-induced chemistry as mentioned earlier. For this reason we refrain from detailed discussion, concluding only that these data provide maximums for these channels and are consistent with our previous observations [1].

4. Conclusions

The most important finding of this Letter is that our studies support the ‘best-fit’ model of 1-pentyl radical decomposition developed in Ref. [1]. In particular the predicted extrapolation with pressure is in excellent agreement with the new data obtained at pressures as high as 5000 kPa. The model and data suggest that the high pressure limiting value of the branching ratio is approached under the conditions of high pressure examined at UIC. The previously tested alternate models that led to much larger high pressure limiting values of the ethene/propene branching ratio can therefore be ruled out. This sets strong limits on the kinetic parameters for the competing reactions. A roughly 60-fold range of pressure has now been covered and includes most of the region of greatest practical interest. Predictions outside of the experimental range, particularly those at higher temperatures and lower pressures, have larger uncertainties and are subject to the limitations of the master equation treatment. The present values should nonetheless be more reliable than those heretofore available.

The predicted pressure dependence is dependent on the selected potential energy surface (PES), as well as the parameters used to describe energy transfer. With the exponential-down model employed, the present data continue to support the energy transfer value estimated earlier [1] on the basis of the NIST data from lower pressures, $\langle\Delta E_{\text{down}}\rangle = (675 \pm 100) \text{ cm}^{-1}$ at 1000 K. It should be noted that the model used for energy randomization within the context of RRKM theory plays a role in our conclusions. We follow the usual procedure wherein molecules are treated as

symmetric tops. The degenerate two dimensional external rotation is then generally considered to be adiabatic, whereas the remaining degree of freedom is allowed to participate in energy exchange [31,33]. Using the PES from our 'best-fit' model, we find that equally good fits are obtained if the degenerate external rotation is also made active, but that the required value of $\langle \Delta E_{\text{down}} \rangle$ (1000 K) is then reduced from 675 cm^{-1} to about 550 cm^{-1} . The data provide no information on which model is to be preferred, but, to the extent that the present results can be extrapolated to other systems, it is important to maintain self-consistency in the RRKM treatment.

Acknowledgments

The authors thank Prof. Kenneth Brezinsky for the generous use of his high pressure shock tube apparatus at the University of Illinois at Chicago. J. A.M. thanks Prof. David M. Golden at Stanford University, CA for suggesting we examine the impact of assumptions regarding adiabatic modes in our RRKM model.

Appendix A. Supplementary data

Supplementary data associated with this article [product data from individual experiments, parameters used in the RRKM/ME analysis, species thermodynamics in NASA polynomial format, and parameters for chemical kinetic modeling from (600–1700) K and (10 to 100000 kPa)] can be found, in the on-line version, at <http://dx.doi.org/10.1016/j.cplett.2012.09.039>.

References

- [1] I.A. Awan, D.R. Burgess Jr., J.A. Manion, J. Phys. Chem. A 116 (2012) 2895.
- [2] L. Endrenyi, D.J. Leroy, J. Phys. Chem. 70 (1966) 4081.
- [3] R.M. Marshall, Int. J. Chem. Kinet. 22 (1990) 935.
- [4] A. Miyoshi, J. Widjaja, N. Yamauchi, M. Koshi, H. Matsui, Proc. Combust. Inst. 29 (2002) 1285.
- [5] K.W. Watkins, Can. J. Chem. 50 (1972) 3738.
- [6] K.W. Watkins, D.R. Lawson, J. Phys. Chem. 75 (1971) 1632.
- [7] N. Yamauchi, A. Miyoshi, K. Kosaka, M. Koshi, N. Matsui, J. Phys. Chem. A 103 (1999) 2723.
- [8] W. Tsang, V. Bedanov, M.R. Zachariah, Ber. Bunsen-Ges. Phys. Chem. 101 (1997) 491.
- [9] S.H. Robertson, M.J. Pilling, L.C. Jitariu, I.H. Hillier, Phys. Chem. Chem. Phys. 9 (2007) 4085.
- [10] L.C. Jitariu, L.D. Jones, S.H. Robertson, M.J. Pilling, I.H. Hillier, J. Phys. Chem. A 107 (2003) 8607.
- [11] J.J. Zheng, D.G. Truhlar, J. Phys. Chem. A 113 (2009) 11919.
- [12] C.J. Hayes, D.R. Burgess Jr., J. Phys. Chem. A 113 (2009) 2473.
- [13] B. Bankiewicz, L.K. Huynh, A. Ratkiewicz, T.N. Truong, J. Phys. Chem. A 113 (2009) 1564.
- [14] A.C. Davis, J.S. Francisco, J. Phys. Chem. A 115 (2011) 2966.
- [15] W.S. McGivern, I.A. Awan, W. Tsang, J.A. Manion, J. Phys. Chem. A 112 (2008) 6908.
- [16] I.A. Awan, W.S. McGivern, W. Tsang, J.A. Manion, J. Phys. Chem. A 114 (2010) 7832.
- [17] I.A. Awan, D.R. Burgess Jr., W. Tsang, J.A. Manion, Int. J. Chem. Kinet. 44 (2012) 351.
- [18] A. Comandini, T. Malewicki, K. Brezinsky, Rev. Sci. Instrum. 83 (2012) 034101.
- [19] R.S. Tranter, R. Sivaramakrishnan, N. Srinivasan, K. Brezinsky, Int. J. Chem. Kinet. 33 (2001) 722.
- [20] R.S. Tranter, K. Brezinsky, D. Fulle, Rev. Sci. Instrum. 72 (2001) 3046.
- [21] W.Y. Tang, K. Brezinsky, Int. J. Chem. Kinet. 38 (2006) 75.
- [22] A. Lifshitz, I. Shweky, J.H. Kiefer, S. Sidhu, in: K. Takayama (Ed.), Shock Waves, Proceedings of the 18th International Symposium on Shock Waves, Sendai, Japan (1991), Springer Verlag, Berlin, 1992, p. 825.
- [23] W. Tsang, A. Lifshitz, Int. J. Chem. Kinet. 30 (1998) 621.
- [24] J.A. Manion, I.A. Awan, Proc. Combust. Inst. 34 (2012) in press, <http://dx.doi.org/10.1016/j.proci.2012.05.078>.
- [25] V. Babushok, T. Noto, D.R.F. Burgess, A. Hamins, W. Tsang, Combust. Flame 107 (1996) 351.
- [26] T. Noto, V. Babushok, A. Hamins, W. Tsang, Combust. Flame 112 (1998) 147.
- [27] J.D. Cox, D.D. Wagman, V.A. Medvedev (Eds.), CODATA Key Values for Thermodynamics, Hemisphere Publishing Corp, New York, 1984.
- [28] V. Mokrushin, V. Bedanov, W. Tsang, M. Zachariah, V.D. Knyazev, W.S. McGivern, ChemRate, National Institute of Standards and Technology, Gaithersburg, Maryland, 1996–2011.
- [29] V.M. Bedanov, W. Tsang, M.R. Zachariah, J. Phys. Chem. 99 (1995) 11452.
- [30] W. Tsang, V. Bedanov, M.R. Zachariah, J. Phys. Chem. A 100 (1996) 4011.
- [31] R.G. Gilbert, S.C. Smith, Theory of Unimolecular and Recombination Reactions, Blackwell Scientific Publications, Oxford, 1990.
- [32] CHEMKIN-PRO. Reaction Design, San Diego, CA USA, 2008.
- [33] K.A. Holbrook, M.J. Pilling, S.H. Robertson, Unimolecular Reactions, second ed., John Wiley & Sons, Chichester, 1996.